# Kinetics Study of Oxidative Desulfurization of Real Diesel Fuel Over Uncoated and Coated Nano-catalysts in an Oscillatory Helical Baffled Reactor

## Amer Nawaf[1] * , Basma Abbas Abdulmajeed[2]

1. College of Petroleum Process Engineering, Tikrit University, Iraq. E-mail: amer.talal@tu.edu.iq
2. Department of chemical engineering, College of engineering, University of Baghdad, Baghdad, Iraq. E-mail: Basma1957@yahoo.com

| ARTICLE INFO | ABSTRACT |
|---|---|
| **Article History**:<br>Received: 04 June 2024<br>Revised: 15 August 2024<br>Accepted: 18 July 2024<br><br>**Article type**: Research<br><br><br>**Keywords**:<br>Mathematical Model,<br>Peracetic Acid,<br>Oscillatory Baffled Reactor,<br>Oxidative Desulfurization | The oxidative desulfurization (ODS) of real diesel fuel (RDF) was evaluated in a modified design oscillatory helical baffled reactor (OHBR). Peracetic acid was produced from hydrogen peroxide and acetic acid and used as an oxidant. Following that, a new design was made using nano-catalyst (uncoated and coated). The experimental work of the oxidative desulfurization process was utilized in an oscillatory helical baffled reactor under moderate conditions: residence times 3-9 min, oxidation temperatures 50-80 ℃, amplitude of oscillation 2-8 mm, and frequency of oscillation 0.5-2 min with 0.4 g of nano-catalyst with constant pressure. The optimal conversion of sulfur was 98.42% for the uncoated catalyst and 96.57% for the coated catalyst under 80 ℃, 8 mm, and 2.5 Hz. The purpose of this manuscript is to determine the ODS kinetic parameters and sulfur compound concentration profile in RDF. The model developed was according to the properties of the real diesel fuel, types of nano-catalysts, and operation conditions inside the OHBR based on the experimental observations. The optimal kinetic model and the half-life period of the nano-composites for the pertinent reactions have also been examined. This study also estimates the best kinetic model parameters of the oxidation reactions using the pseudo-first-order technique, which is based on the experimental data. |

## Introduction

The world's demand for feedstock (such as crude oil) at a low price of energy has grown, and it is predicted to proceed at the current rate until 2035. Crude oil has been considered the most important energy source in the world for a long time. Therefore, crude oil represents a crucial role in the global energy resource, because of the global energy requirement. Due to depleting fossil fuel sources and increasing energy demand, low-quality fossil fuels (diesel fuel) have become inevitable [1, 2].

The classification of crude oil is represented by liquid, gaseous, and solid compounds, including oxygen, sulfur, nitrogen, and minimum quantities of metals represented by copper, nickel, iron, and others that may be found in refined specialty end-products like light and heavy diesel, and jet fuel [3, 4]. Crude oil compounds are represented by hydrocarbons like

heteroatoms, aromatic rings, and straight chains. Following that, transportation fuels such as gasoline, diesel (light and heavy), and jet fuel were classified as the most important portion of crude oil. The sulfur compounds and American Petroleum Institute (API) gravity are considered the most important properties of crude oil [5, 6]. The decline in the exploration and production of crude oil reserves worldwide indicates a global dependence on heavier crude oils that contain heteroatoms like organic sulfur [7]. Therefore, the amount of sulfur in petroleum refinery streams is growing significantly (i.e., increasing sulfur percent). Burning liquid fuels produced from low-quality fuel feedstocks results in increased external nitrogen monoxide and sulfur dioxide emissions [8, 9]. Therefore, sulfur removal from crude oil is necessary for industrial and environmental reasons.

In world demand, the new technology for sulfur removal, the oxidative desulfurization (ODS) method, has been most effective toward the sulfur compounds, especially thiophene and its derivatives in diesel fuel. The ODS technology can obtain ultra-deep desulfurization with low cost based on moderate operating conditions such as residence time and oxidation temperature under 1 atm, efficient catalysts, and without using hydrogen in the process [10-12]. The ODS process is conducted utilizing different oxidant agents such as oxygen [13], hydrogen peroxide [14], hydrogen peroxide/acetic acid [15], and air [16]. Peracetic acid (hydrogen peroxide/acetic acid) is used due to its availability, easy formation, low cost, high oxidant, and absence of environmental effluent. According to published research, peracetic acid ($CH_3CO_3H$) increased the number of hydroperoxides produced in situ, accelerating the rate at which sulfur compounds were converted to sulfoxides and/or sulfones [17].

Abdulateef et al. examined the oxidative desulfurization process (ODS) of the simulated fuel (LGO-DBT) applied modified synthesis AgO-ZnO/HY-zeolite bimetallic nano-catalyst and air as an oxidant utilizing a batch reactor under conditions of reaction temperatures 115-165 °C, sulfur content 1200 ppm, and catalyst doses of 0.4-1.4 g, under constant pressure of 1 amt. The results of this research concluded that optimal sulfur conversion was 91.8% [18].

Cao et al. investigated the aerobic oxidative desulfurization (AODS) of model oil fuel (BT, DBT, and 4,6-DMDBT) utilizing flower-like cobalt–molybdenum mixed-oxide microspheres (CoMo-FMs) as catalyst and $O_2$ as oxidant under a temperature range of 80-110 °C, in a batch reactor. It showed the high efficiency of the catalyst in reducing the sulfur compounds in the model fuel at a temperature of reaction 100 °C and a time of reaction of 90 minutes [19].

Hameed et al. investigated the oxidation reaction of light gas oil using (CuO/AC) as a catalyst and $H_2O_2$ as an oxidant in a newly designed digital baffle batch reactor (DBBR). From the experimental work, it was found that increased sulfur conversion was accomplished when temperature increased. The present work conducted an oxidative desulfurization process (ODS) of real diesel fuel in an oscillatory helical baffled reactor (OHBR-pilot plant). The reactor was used to obtain the kinetic parameters of an ODS process over an uncoated and coated nano-catalyst. This new model is based on the parameter of the OHBR unit and based on real diesel fuel cuts [20].

## Experimental Work and Materials Used

### Materials Used

The feedstock applied in the experimental work was the real diesel fuel cut that was obtained from the Iraqi Ministry of Oil: Refineries. The details of the real diesel fuel are shown in Table 1.

**Table 1**. The physical properties of real diesel fuel utilized in the manufacturing.

| Physical properties | Value |
| --- | --- |
| Sulfur content | 464.13 ppm |
| Diesel-color | 0.5 |
| Density | 0.8214 @15 °C |
| Flash point | 64.2 °C |
| API | 40.76 |
| Viscosity | 2 @ 40 °C (Cst) |
| Pour point (°C) | -18 |
| content of water | 37.9 |
| Initial boiling point (°C) | 182 |
| 5% | 190 |
| 10% | 201 |
| 20% | 203 |
| 30% | 210 |
| 40% | 221 |
| 50% | 235 |
| 60% | 252 |
| 70% | 268 |
| 80% | 302 |
| 90% | 318 |
| 100% | 345 |
| T. D | 97% |
| Loss | 2 |
| Res. | 1 |

50% hydrogen peroxide ($H_2O_2$) and acetic acid ($CH_3CO_2H$) obtained from Merck Millipore /Germany, J.T.Baker/United States, respectively, are used to produce peracetic acid ($CH_3CO_3H$) to apply as an oxidizing agent to oxidize sulfur compound in real diesel fuel. The specifications of support used in the prepared uncoated and coated nano-catalyst are shown in Table 2.

**Table 2**. The specification of composite support ($\gamma$-$Al_2O_3$-$TiO_2$) used in the nano-catalyst prepared

| Composite support properties | Value |
| --- | --- |
| Percent of $\gamma$-alumina | 75% |
| Percent of $TiO_2$ | 25% |
| Surface area ($m^2/g$) | 153.97 |
| Pore volume ($cm^3/g$) | 0.2132 |
| Relative crystallinity | 84% |

## Preparation of Nano-catalyst

The composite support ($\gamma$-$Al_2O_3$-$TiO_2$) was impregnated with 5% iron by incipient wetness impregnation (IWI) [21-24]. The salt solution of Fe metal was prepared by dissolving 1.7217 g of ferric nitrate salt ($Fe(NO_3)_3.9H_2O$) in 50 ml of double-deionized water (DDW) and magnetic stirring (650 rpm) to obtain a clear iron solution. The dry composite support particles, 2.7 g, were placed in a conical (100 ml), and a funnel was utilized to add the impregnation solution (salt solution) drop-by-drop with increasing the stirring by a magnetic stirrer up to 850 rpm (to increase the homogeneity). The impregnated composite support was further mixed in an ultrasonic sonicator (Toption, designed in China, model: LC-JY92-IIN) for 5 hr to increase impregnation. The solution was heated in the electrical oven at 110 °C, until all solvent was evaporated. The wet ($Fe_2O_3/\gamma$-$Al_2O_3$-$TiO_2$) was placed in a tubular furnace (China, Safe-therm, China). Then, the sample was calcined at a range of temperatures (150 °C at 1 h, 250 °C at 1hr, 400 °C at 1.5 hr and 570 °C at 2.5 hr), at a heating rate of 5 °C/min under constant oxygen flow rate of 1 ml/min obtained by $O_2$ generation (650 W and NG-300P) to boost conversion of the iron salt to iron oxides.

## Coating Synthesis for Nano-catalyst

Firstly, dry the nano-catalyst at 150 ℃ for 3 hours in an electric oven before using. The salt solution of Mn metal was prepared by dissolving 0.15 g of manganese acetate Mn $(CH_3CO_2)_2$. $H_2O$ salt in 20 ml of absolute ethanol and stirred using magnetic stirring at 350 rpm to obtain a clear solution of manganese. Second step (coating step): the dry nano-catalyst ($Fe_2O_3$/γ-alumina-$TiO_2$) particles, 1.7 g, were placed in a conical flask (50 ml), and a funnel was utilized to add the impregnation solution (manganese solution) drop-by-drop with stirring by magnetic stirring at 350 rpm. The solution was then transferred to the ultrasonic homogenizer sonicator processor mixer at (65% power rate, 3 pulses-OFF, 5 pulses-ON, for 100 minutes, the sample was left to rest for 5 hours). After that, the sample was transferred to an electrical oven at 60 ℃ until all the ethanol was evaporated. The sample was calcinated under an atmosphere in the tubular furnace at a heating rate of 10 °C/min for 3 hours at a calcinated temperature of 550 ℃ to form the Mn-($Fe_2O_3$/γ-alumina-$TiO_2$) coating layer. Finally, the coating layer formed at 1.5%.

## Experimental Setup

Figs. 1 & 2, showed a pilot plant and a schematic diagram of the experimental unit utilized for oxidative desulfurization of the real diesel fuel in an oscillatory helical baffled reactor. The real fuel (diesel cut) was stored in tank1 and flown to the tubular reactor by pump1 (net flow: MFG. NO. 5228 Taiwan). The flow rate of the feedstock was adjusted and oscillated via pump 2 (local design). The volume of the flown feedstock was used to adjust the oscillation amplitude to achieve the desired oscillation amplitude by shifting the plunger, while the oscillation frequency was adjusted by setting the voltage of the pump 2 that connects the pump to the feedstock tank. The peracetic acid was fed through a mass flow meter and delivered to the bottom of the OHBR. To generate the oscillatory eddies inside the tubular reactor, a second pump 2 was used for this purpose. It is connected to the tubular reactor via a stainless-steel tube and a customized union.



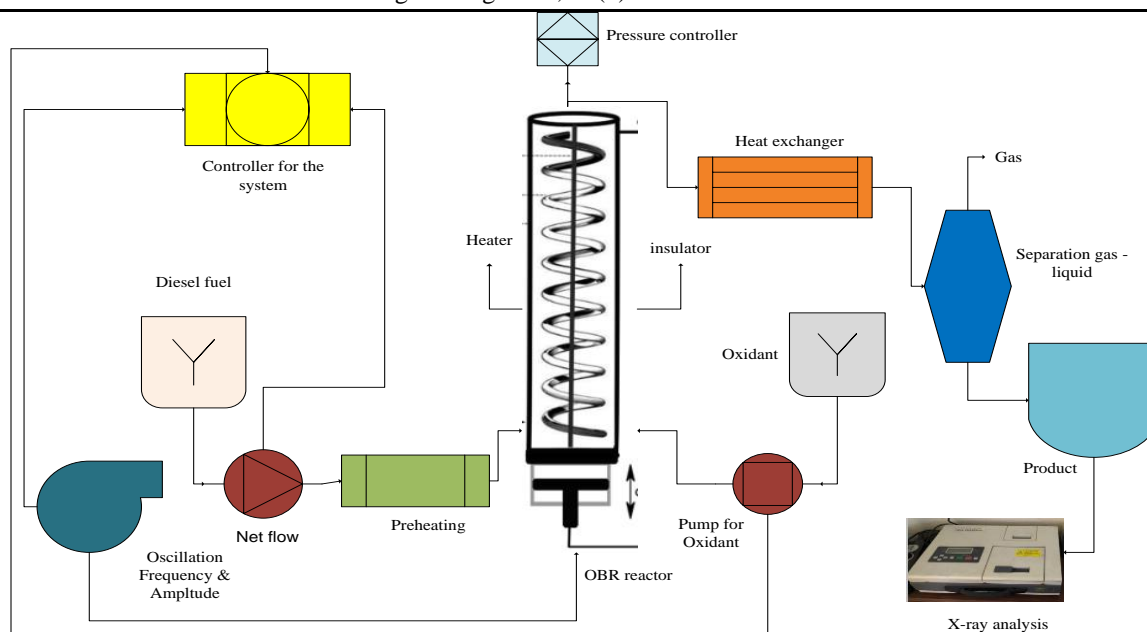**Fig. 1**. Design of the oscillatory helical baffled reactor (OHBR)

**Fig. 2**. Schematic diagram of the oscillatory helical baffled reactor

## Product Analysis

The desulfurized real diesel fuel samples were withdrawn to determine the total sulfur content by X-ray sulfur analyzer (0.15-3000 ppm, 50Hz, 220V, Ankara-Turkey) in the laboratory of the north refineries company in Iraq (Sallah-Aldeen/Baiji) based on ASTM D7039 standards. During the ODS process, the desulfurization efficiency of sulfur compounds was calculated using the following equation:

$$Sulfur\ conversion = \left[\frac{S_f - S_p}{S_f}\right] 100\% \tag{1}$$

where $S_s$ and $S_p$ are sulfur concentrations for inlet and product in ppm.

## Results and Discussions

Fig. 3 shows the FESEM images for the uncoated nano-catalyst, which showed excellent dispersion of the metal oxide on the composite support. Furthermore, $Fe_2O_3$ particles were well-deposited on the surface of the composite without any agglomeration [25]. Consequently, the surface area and pore volume of the nano-catalyst maintained high values after loading metal oxide (140.29 $m^2$/g, 0.1339 $cm^3$/g), respectively. Also, this indicated a good IWI procedure for preparing the nano-catalyst. The TEM results for the coated nano-catalyst, as shown in Fig. 4, showed the TEM morphology of the manganese acetate coating film and $Fe_2O_3$/γ-alumina-$TiO_2$ substrate (as marked by the black arrows). TEM observation reveals that a layer surrounds the nano-catalyst particle. These layers are transparent layers of Mn formed as a result of the coating process, which observes the success of the coating process of the $Fe_2O_3$/γ-alumina-$TiO_2$ substrate. It appeared that the coating film's thickness was made up of two distinct particle sizes (50 and 500 nm) as indicated by the black arrow and with the use of Image J software.
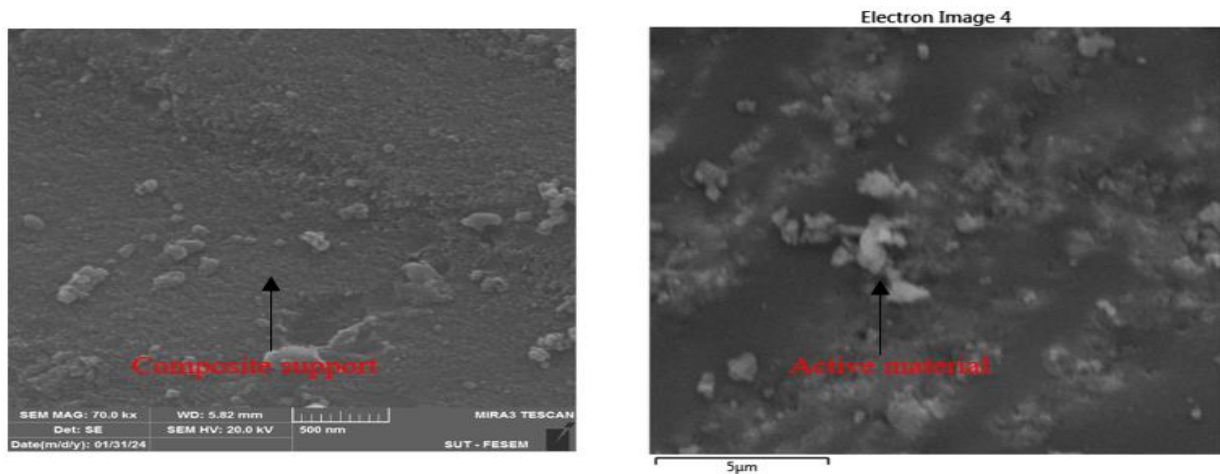
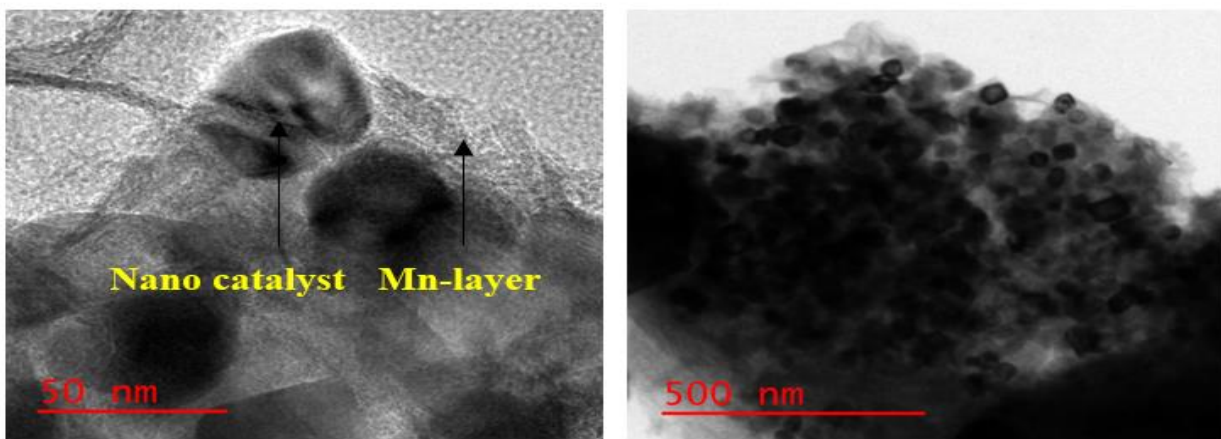**Fig. 3**. FESEM results for composite support and uncoated nano-catalyst
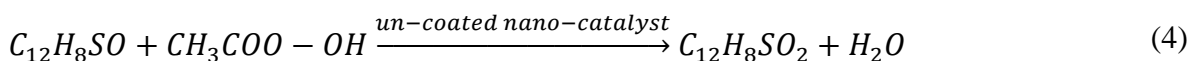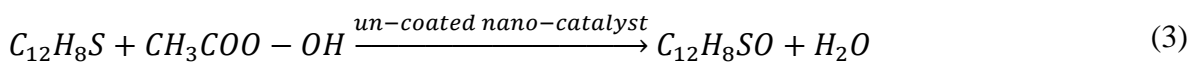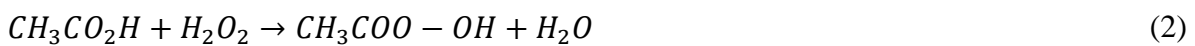


**Fig. 4**. TEM results for coated nano-catalyst

ODS works by oxidizing real diesel fuel (RDF) with peracetic acid in multiple steps, forming polar sulfoxides/or sulfones through a free radical mechanism. Hydrogen peroxide and acetic acid (1.4 ml $H_2O_2/CH_3CO_2H$) are mixed to form peracetic acid with concerning Eq. 2. Eqs. 3-5 represent the reactions that occur when sulfur compounds are oxidized by peracetic acid in the presence of an un-coated and coated nano-catalyst, resulting in the formation of sulfoxide (DBTO) and sulfone (DBTO$_2$):

$$CH_3CO_2H + H_2O_2 \rightarrow CH_3COO - OH + H_2O \tag{2}$$

$$C_{12}H_8S + CH_3COO - OH \xrightarrow{un-coated\ nano-catalyst} C_{12}H_8SO + H_2O \tag{3}$$

$$C_{12}H_8SO + CH_3COO - OH \xrightarrow{un-coated\ nano-catalyst} C_{12}H_8SO_2 + H_2O \tag{4}$$

The overall oxidation reaction is given by the following reaction:

$$C_{12}H_8S + 2CH_3COO - OH \xrightarrow{un-coated\ nano-catalyst} C_{12}H_8SO_2 + H_2O \tag{5}$$
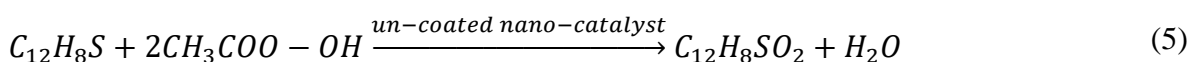
From experimental results, it was found that all parameters, such as oscillation frequency, oscillation amplitude, residence times, and temperature of oxidation, affected the removal of sulfur [26-29], as shown in Fig. 5. Peracetic acid is formed through the mixing of oxidant (1.4 ml $H_2O_2$/$CH_3CO_2H$). It was observed that the conversion of sulfur rapidly increased from 54.98% to 78.00% by raising the oxidation time from 3 to 6 min, for uncoated nano-catalyst. The elimination was enhanced from 52.82% to 75.64% when the oxidation time was extended from 3 to 6 min for the coated nano-catalyst, as shown in Fig. 5.

The reason for this decrease in removal is dependent on the deactivation of the nano-catalyst due to sulfur deposition on pores (i.e., the porosity of nano-catalyst) with time, and this is one of the challenges facing the use of plain noble metal (as a coating layer) [30]. Also, it was found that the drop in removal for the coated composite was slightly smaller than that for the uncoated nano-composite, and this indicates that the coating material (Mn) acted as a protective layer for preventing nano-catalyst deactivation and prolonging the deactivation time of the nano-catalyst [31].
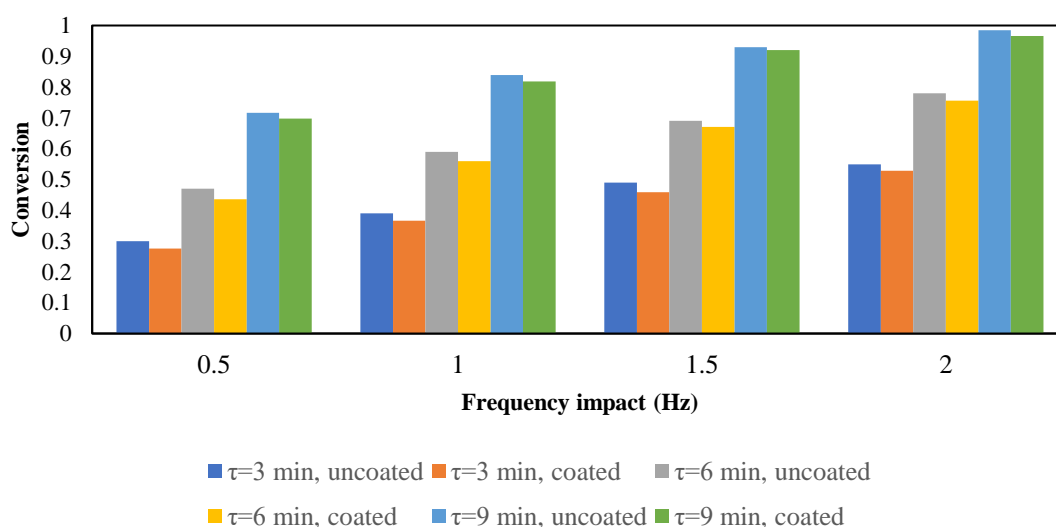


**Fig. 5**. Effect of frequency of oscillation and residence time on ODS process for uncoated and coated nano-catalyst at an amplitude of oscillation 8 mm and oxidation temperature 80 °C under atmosphere pressure

## Mathematical Modeling of Oxidation Desulfurization Process (ODS) in OHBR

### Mathematical Modeling of Oxidation Reaction for Uncoated and Coated Nano-catalyst

The following assumptions were applied in the development of the present model for the ODS process using OHBR design [21, 28]:
1. The state of OHBR is batch mode.
2. The reaction inside the pilot plant (OHBR) is heterogeneous.
3. Peracetic acid produced from the material is of high purity and used as an oxidant.
4. The products and feed of real diesel fuel are in the liquid phase.
5. Constant pressure and isothermal operation of the OHBR unit.
6. Perfect mixing inside the tubular reactor by oscillation (frequency and amplitude).

The kinetics model connected to the (ODS) process is tested here with peracetic acid ($CH_3CO_3H$) as the oxidant for the nano-catalysts prepared (uncoated and coated), including pseudo-first and second-order kinetics, internal particle diffusion model and external diffusion model which are communicated inside the kinetic oxidation rate equation (represented below)

to determine the excellent kinetic model by comparing the correlation coefficients among them, are modeled here.

The mole balance equation on the batch system for the oscillatory helical baffled reactor (OHBR) for the ODS process can be explained as [32-34]:

$$[Inlet] = [Outlet] + [Accumulation] + [Dissapparance \ by \ oxidation] \tag{6}$$

The chemical materials (real diesel fuel, peracetic acid, uncoated, and coated nano-catalyst) in the input and output for OHBR are equal to zero. Therefore, Eq. 6 becomes:

$$[Inlet \ diesel \ mole \ ] = [Outlet \ diesel \ mole] = 0 \tag{7}$$

Following that, the product from Eq. 7 and the substitution in Eq. 6 result in the formula that follows:

$$-[Dissapparance \ by \ oxidation] = [Accumulation \ of \ oxidation] \tag{8}$$

Through the oxidative desulfurization process, the oxidation reaction can evaluate the significance of the response disappearance and the oxidation reaction accumulation, represented below [32]:

$$Accumulation \ of \ oxidation \ reaction = -([R_S][V_{Reactor}])_{in \ OHBR} \tag{9}$$

$$Dissapparance \ of \ oxidation \ reaction = \left(\frac{dN_S}{d\tau}\right)_{in \ OHBR} \tag{10}$$

Where, $V_{OHBR}$ indicates the volume of the oxidation reaction (i.e., the same volume of OHBR), $R_S$ represents the oxidation reaction rate of the ODS technology. Substitution, Eqs. 9 & 10 in Eq. 8, the reaction rate of oxidative desulfurization process at steady density (no change in volume and constant pressure) is obtained:

$$-[R_S][V_{OHBR}] = -\left[\frac{dN_S}{d\tau}\right] \tag{11}$$

After that, arrangement of the Eq. 11 is represented as follows:

$$-[R_S] = -\left[\frac{d(\frac{N_S}{V_{OHBR}})}{d\tau}\right] \tag{12}$$

$$-[R_S] = -\left[\frac{dC_S}{d\tau}\right] \tag{13}$$

The chemical oxidation reaction rate is represented as follows:

$$for \ Pseudo \ order \ equation \ of \ ODS = -[R_S] = KC_S^n \ C_{peracetic \ acid}^m \tag{14}$$

The concentration of oxidant ( $C_{peracetic \ acid}^m$ ) and constant reaction rate ($K$) equal to the apparent rate constant ( $K_{app.}$) can be represented as [35]:

$$K_{app.} = K \ C_{peracetic \ acid}^m \tag{15}$$

First, assuming the $K_{app.} = K_p$ and in the pseudo-first order oxidation reaction (n = 1) and from Eq. 15, Eq. 14 can be rearranged to be:

$$-[R_S] = K_p \, C_S \tag{16}$$

$$-\left[\frac{dC_S}{d\tau}\right] = K_p \, C_S \tag{17}$$

The Eq. 17 can be rearranged and become, as shown below:

$$\int_{C_{S_0}}^{C_{S_{final}}} \frac{dC_S}{C_S} = -\int_0^\tau K_p \, d\tau \tag{18}$$

$$ln\frac{C_{S_0}}{C_{S_{final}}} = K_p \, \tau \tag{19}$$

Second, in the pseudo-second-order oxidation reaction (n = 2), the following reaction rate equation for the ODS process can be noticed below:

$$-\frac{dC_S}{d\tau} = -[R_S] = K_p \, C_S^2 \tag{20}$$

$$-[R_S] = K_p \, C_S^2 \tag{21}$$

$$\int_{C_{S_0}}^{C_{S_{final}}} \frac{dC_S}{C_S^2} = \int_0^\tau K_p \, d\tau \tag{22}$$

The pseudo-second-order reaction's final expression can be expressed as:

$$\frac{1}{C_{S_{final}}} - \frac{1}{C_{S_0}} = K_p \, \tau \tag{23}$$

**Kinetic Model for Oxidation Desulfurization over Uncoated and Coated Nano-catalysts**

The oscillation of flow (frequency and amplitude) can impact sulfur conversion found in real diesel fuel (RDF) at different oxidation temperatures, residence times, and constant amounts of nano-catalysts (uncoated and coated). Based on the pseudo-first and second-order kinetics models, the oxidation reaction rate constants have been evaluated at different oxidation temperatures and oscillations (frequency and amplitude). In the oxidation, the comparison between the first and second kinetic models for the oxidative desulfurization reaction employing uncoated and coated nano-catalysts is shown in Tables 3a & 3b to give further insight into the process. Based on the findings displayed in these Tables, it has been observed that the oxidation reactions of RDF using the synthesized uncoated and coated nano-catalysts are followed by the pseudo-first-order kinetics, giving a better fit than pseudo-second-order kinetics [32].

**Table 3a**. Kinetic model result for ODS using uncoated nano-catalyst at residence time 9 min

| Nano-catalyst | Order of Oxidation Reaction | Temperature of Oxidation, °C | Rate Constant $(Con)^{1-n} (min)^{-1}$ | Oscillation of Flow |
|---|---|---|---|---|
| Uncoated nano-catalyst | Pseudo first order | 50 | $9.9097*10^{-2}$ | Frequency = 0.5 Hz |
| | | 65 | $1.2011*10^{-1}$ | |
| | | 80 | $1.4024810^{-1}$ | |
| | | 50 | $1.1982*10^{-1}$ | Frequency = 1 Hz |
| | | 65 | $1.4489*10^{-1}$ | |
| | | 80 | $2.0309*10^{-1}$ | |
| | | 50 | $1.4186*10-1$ | Frequency = 1.5 Hz |
| | | 65 | $1.8430*10^{-1}$ | |
| | | 80 | $2.9547*10^{-1}$ | |
| | | 50 | $1.5861*10^{-1}$ | Frequency = 2 Hz |
| | | 65 | $2.1962*10^{-1}$ | |
| | | 80 | $4.6075*10^{-1}$ | |
| | Pseudo second order | 50 | $1.6435*10^{-3}$ | Frequency = 0.5 Hz |
| | | 65 | $4.6629*10^{-4}$ | |
| | | 80 | $6.0645*10^{-4}$ | |
| | | 50 | $4.6446*10^{-4}$ | Frequency = 1 Hz |
| | | 65 | $6.4257*10^{-4}$ | |
| | | 80 | $1.2486*10^{-3}$ | |
| | | 50 | $6.1886*10^{-4}$ | Frequency = 1.5 Hz |
| | | 65 | $1.0180*10^{-3}$ | |
| | | 80 | $3.1804*10^{-3}$ | |
| | | 50 | $7.5854*10^{-4}$ | Frequency = 2 Hz |
| | | 65 | $1.4886*10^{-3}$ | |
| | | 80 | $1.4898*10^{-2}$ | |

**Table 3b**. Kinetic model result for ODS using coated nano-catalyst at residence time 9 min

| Nano-catalyst | Order of oxidation reaction | Temperature of oxidation, °C | Rate constant $(Con)^{1-n}$ $(min)^{-1}$ | Oscillation of flow |
|---|---|---|---|---|
| Coated nano-catalyst | Pseudo first order | 50 | $9.5966*10^{-2}$ | Frequency = 0.5 Hz |
| | | 65 | $1.1802*10^{-1}$ | |
| | | 80 | $1.4024*10^{-1}$ | |
| | | 50 | $1.1450*10^{-1}$ | Frequency = 1 Hz |
| | | 65 | $1.3842*10^{-1}$ | |
| | | 80 | $1.8949*10^{-1}$ | |
| | | 50 | $1.3448*10^{-1}$ | Frequency = 1.5 Hz |
| | | 65 | $1.7042*10^{-1}$ | |
| | | 80 | $2.8077*10^{-1}$ | |
| | | 50 | $1.5686*10^{-1}$ | Frequency = 2 Hz |
| | | 65 | $2.1586*10^{-1}$ | |
| | | 80 | $3.7470*10^{-1}$ | |
| | Pseudo second order | 50 | $3.2843*10^{-4}$ | Frequency = 0.5 Hz |
| | | 65 | $4.531*10^{-4}$ | |
| | | 80 | $5.535*10^{-4}$ | |
| | | 50 | $4.3155*10^{-4}$ | Frequency = 1 Hz |
| | | 65 | $5.9270*10^{-4}$ | |
| | | 80 | $1.0781*10^{-3}$ | |
| | | 50 | $5.6367*10^{-4}$ | Frequency = 1.5 Hz |
| | | 65 | $8.7046*10^{-4}$ | |
| | | 80 | $2.7568*10^{-3}$ | |
| | | 50 | $7.4294*10^{-4}$ | Frequency = 2 Hz |
| | | 65 | $1.4312*10^{-3}$ | |
| | | 80 | $6.7400*10^{-3}$ | |

**Half-live Period for Uncoated and Coated Nano-catalyst**

From Nano-composites ($Fe_2O_3/\gamma\text{-}Al_2O_3\text{-}TiO_2$ and Mn-coated $Fe_2O_3/\gamma\text{-}Al_2O_3\text{-}TiO_2$) designed in this study, the half-live period ($t_{1/2}$) is also determined for each nano-catalyst via utilizing the following equations at the operating conditions (residence time 9 min, oxidation temperature 80 °C, amplitude of oscillation 8 mm, and frequency of oscillation 2 Hz) with constant pressure:

Uncoated nano-catalyst: $t_{1/2} = \frac{ln2}{K} = \frac{0.6931}{0.46075} = 1.504$ min      (24)

Coated-nano catalyst: $t_{1/2} = \frac{ln2}{K} = \frac{0.6931}{0.3747} = 1.8497$ min      (25)

The half-life period of the sulfur oxidative desulfurization process was 4.0221 and 1.8497 min for uncoated and coated nano-catalysts, respectively [32]. The weight ratio of real diesel fuel to nano-catalyst was about 250/0.4 for all nano-composites synthesized separately. Consequently, it was further considered that the adsorption and diffusion on the kinetic model affect sulfur removal through the oxidative desulfurization process. Such an impact of the oxidation diffusion process was disregarded in the public domain.

**The Oxidative Reaction's Activation Energy in OHBR**

From the Arrhenius equation, the activation energy can be evaluated, as shown below [36, 37]:

$$K = A_o Exp\left[-\frac{E_A}{RT}\right]$$      (26)

$$lnK = lnA_o - \left[\frac{E_A}{RT}\right] \tag{27}$$

Following that, a scheme of $1/T(K)$ against ln $K$ will give a straight line with a slope equal to $-EA/R$, where EA activation energy and $(R)$ gas constant are then linearly examined [38], as shown in Figs 6 & 7, for uncoated and coated nano-catalyst, respectively. The values of these nano-catalysts' activation energies for the applicable reactions are 33.36 and 33.36 KJ/mol, for uncoated $Fe_2O_3/\gamma$-$Al_2O_3$-$TiO_2$, and Mn-coated $Fe_2O_3/\gamma$-$Al_2O_3$-$TiO_2$, respectively. It is certainly noticed, according to the results, that the activation energy is the same as that of the prepared nano-catalysts (uncoated and coated) giving a maximum $EA$ for such oxidation reactions tested here, demonstrating that the novel nano-composite synthesized in this manuscript can be confidently applied to the design of reactor, control, and operation.
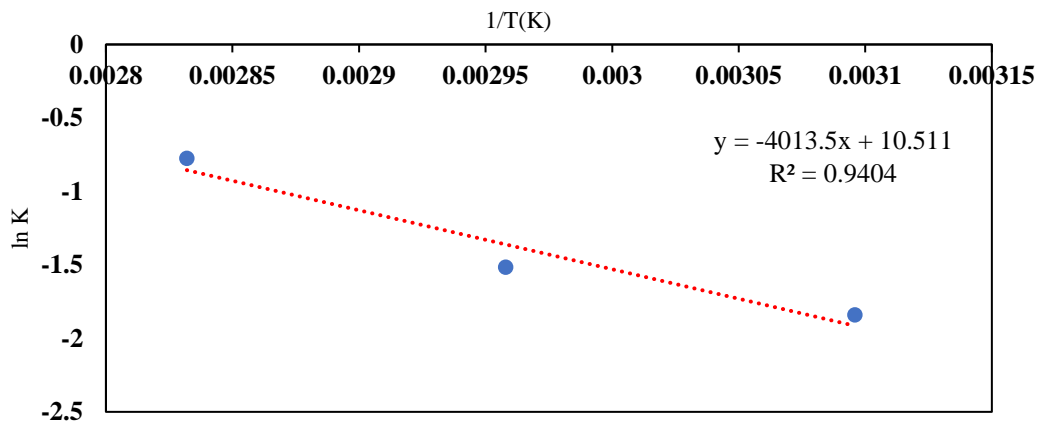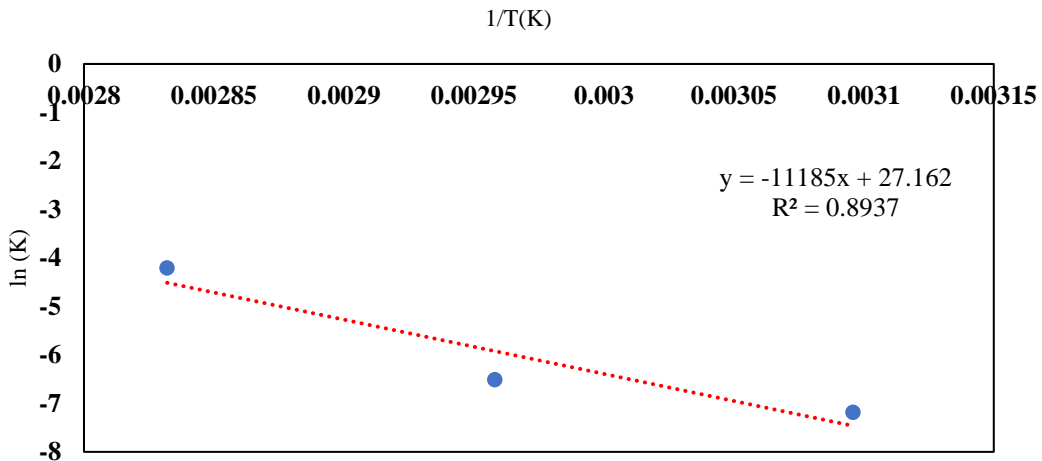


Fig. 6. ln K versus 1/ T of oxidation reaction for uncoated nano-catalyst (a) first order (b) second order
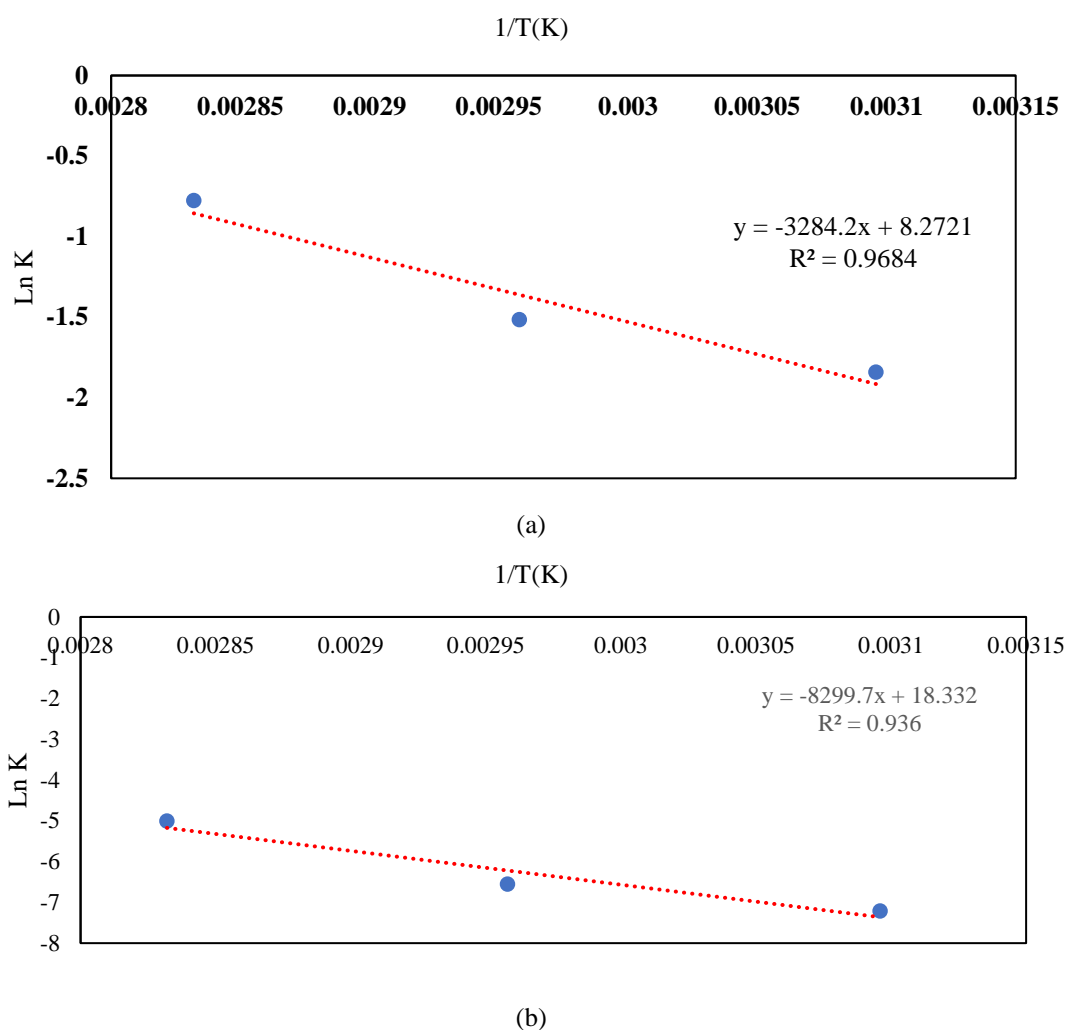
(a)



(b)

**Fig. 7**. ln K versus 1/T of oxidation reaction for coated nano-catalyst (a) first order (b) second order

## Conclusion

To develop increasingly productive innovations on new oxidative nano-catalysts, researchers in this field must continue to face challenges to obtain a suitable catalyst for such impurity-creating clean fuel. So, the novel composite nano-catalyst ($Fe_2O_3$) over composite $\gamma$-$Al_2O_3$-$TiO_2$ nanoparticles is extensively studied here for this purpose via oxidative desulfurization process in a new design oscillatory helical baffled reactor utilizing the peracetic acid as the oxidant.

According to the results reported in this manuscript, the novel uncoated and coated nano-catalyst $Fe_2O_3$/$\gamma$-$Al_2O_3$-$TiO_2$ can be used confidently for ODS reactions, and it has been reported to be one of the most significant catalysts to get clean fuel and decreasing the compounds of sulfur by peracetic acid under moderate operating conditions such as (oscillation frequency, oscillation amplitude, residence times, and the reaction temperature). In the catalyzed process of the oxidation reaction, it was observed that utilizing composite support for the preparation of the nano-catalyst exhibits high effectiveness. The procedure of IWI (impregnation) is an excellent way to prepare nano-catalysts due to the good distribution of iron oxides, in addition to the high pore volume and surface area. The maximum removal of sulfur compounds present in RDF (98.42%) was over uncoated nano-catalyst under the conditions of amplitude = 8 mm, frequency = 2 Hz, oxidation temperature = 80 ℃, and residence time = 9 min). While over the coated nano-catalyst 96.57% at the same conditions. The finest kinetics model connected to the ODS process has been tested here based on peracetic acid ($CH_3CO_3H$)

as an oxidant for coated and uncoated nano-catalysts. A pseudo-first-order kinetics model has been recorded for the ODS reaction, which can show the pilot plant (OHBR).

# References

[1]     Mjalli FS, Ahmed OU, Al-Wahaibi T, Al-Wahaibi Y, AlNashef IM. Deep oxidative desulfurization of liquid fuels. Reviews in Chemical Engineering. 2014 Aug 1;30(4):337-78. https://doi.org/10.1515/revce-2014-0001

[2]     Nawaf AT, Gheni SA, Jarullah AT, Mujtaba IM. Improvement of fuel quality by oxidative desulfurization: Design of synthetic catalyst for the process. Fuel Processing Technology. 2015 Oct 1;138:337-43. https://doi.org/10.1016/j.fuproc.2015.05.033

[3]     El-Gendy NS, Speight JG. Handbook of refinery desulfurization. CRC Press; 2015 Sep 18.

[4]     Shafiq I, Shafique S, Akhter P, Yang W, Hussain M. Recent developments in alumina supported hydrodesulfurization catalysts for the production of sulfur-free refinery products: A technical review. Catalysis Reviews. 2022 Jan 2;64(1):1-86. https://doi.org/10.1080/01614940.2020.1780824

[5]     Speight JG. The desulfurization of heavy oils and residua. CRC Press; 1999 Nov 5.

[6]     Srivastava VC. An evaluation of desulfurization technologies for sulfur removal from liquid fuels. Rsc Advances. 2012;2(3):759-83. https://doi.org/10.1039/C1RA00309G

[7]     Dhir S, Uppaluri R, Purkait MK. Oxidative desulfurization: Kinetic modelling. Journal of hazardous materials. 2009 Jan 30;161(2-3):1360-8. https://doi.org/10.1016/j.jhazmat.2008.04.099

[8]     Houda S, Lancelot C, Blanchard P, Poinel L, Lamonier C. Oxidative desulfurization of heavy oils with high sulfur content: A review. Catalysts. 2018 Aug 23;8(9):344. https://doi.org/10.3390/catal8090344

[9]     Marafi A, Albazzaz H, Rana MS. Hydroprocessing of heavy residual oil: Opportunities and challenges. Catalysis today. 2019 Jun 1;329:125-34. https://doi.org/10.1016/j.cattod.2018.10.067

[10]   Julião D, Valença R, Ribeiro JC, de Castro B, Balula SS. Efficient eco-sustainable ionic liquid-polyoxometalate desulfurization processes for model and real diesel. Applied Catalysis A: General. 2017 May 5;537:93-9. https://doi.org/10.1016/j.apcata.2017.02.021

[11]   Li J, Yang Z, Li S, Jin Q, Zhao J. Review on oxidative desulfurization of fuel by supported heteropolyacid catalysts. Journal of Industrial and Engineering Chemistry. 2020 Feb 25;82:1-6. https://doi.org/10.1016/j.jiec.2019.10.020

[12]   Mahmood QA, Abdulmajeed BA, Haldhar R. Oxidative Desulfurization of Simulated Diesel Fuel by Synthesized Tin Oxide Nano-Catalysts Support on Reduced Graphene Oxide. Iraqi Journal of Chemical and Petroleum Engineering. 2023 Dec 30;24(4):83-90. https://doi.org/10.31699/IJCPE.2023.4.8

[13]   Liu H, Min E. Catalytic oxidation of mercaptans by bifunctional catalysts composed of cobalt phthalocyanine supported on Mg–Al hydrotalcite-derived solid bases: effects of basicity. Green Chemistry. 2006;8(7):657-62. https://doi.org/10.1039/B603461F

[14]   Fathi MI, Humadi JI, Mahmood QA, Nawaf AT, Ayoub RS RS. Improvement of design synthetic nano-catalysts for performance enhancement of oxidative desulfurization using batch reactor. InAIP Conference Proceedings 2022 Nov 17 (Vol. 2660, No. 1). AIP Publishing. https://doi.org/10.1063/5.0109089

[15]   Rezvani MA, Aghmasheh M. Synthesis of t-B. PWFe/NiO nanocomposite as an efficient and heterogeneous green nanocatalyst for catalytic oxidative-extractive desulfurization of gasoline. Environmental Progress & Sustainable Energy. 2021 Jul;40(4):e13616. https://doi.org/10.1002/ep.13616

[16]     Abdulateef LT, Nawaf AT, Mahmood QA, Dahham OS, Noriman NZ, Shayfull Z. Preparation, characterization and application of alumina nanoparticles with multiple active component for oxidation desulfurization. InAIP Conference Proceedings 2018 Nov 9 (Vol. 2030, No. 1). AIP Publishing. https://doi.org/10.1063/1.5066672

[17]     Rezvani MA, Shaterian M, Aghbolagh ZS, Akbarzadeh F. Synthesis and characterization of new inorganic-organic hybrid nanocomposite PMo11Cu@ MgCu2O4@ CS as an efficient heterogeneous nanocatalyst for ODS of real fuel. ChemistrySelect. 2019 May 31;4(20):6370-6. https://doi.org/10.1002/slct.201900202

[18]     Abdulateef LT, Nawaf AT, Al-Janabi OY, Foot PJ, Mahmood QA. Batch oxidative desulfurization of model light gasoil over a bimetallic nanocatalyst. Chemical Engineering & Technology. 2021 Sep;44(9):1708-15. https://doi.org/10.1002/ceat.202100027

[19]     Cao X, Tong R, Wang J, Zhang L, Wang Y, Lou Y, Wang X. Synthesis of Flower-Like Cobalt–Molybdenum Mixed-Oxide Microspheres for Deep Aerobic Oxidative Desulfurization of Fuel. Molecules. 2023 Jun 28;28(13):5073. https://doi.org/10.3390/molecules28135073

[20]     Nawaf AT, Jarullah AT, Abdulateef LT. Design of a synthetic zinc oxide catalyst over nano-alumina for sulfur removal by air in a batch reactor. Bulletin of Chemical Reaction Engineering & Catalysis. 2019;14(1):79. https://doi.org/10.9767/bcrec.14.1.2507.79-92

[21]     Nawaf AT, Jarullah AT, Gheni SA, Mujtaba IM. Development of kinetic and process models for the oxidative desulfurization of light fuel, using experiments and the parameter estimation technique. Industrial & Engineering Chemistry Research. 2015 Dec 23;54(50):12503-15. https://doi.org/10.1021/acs.iecr.5b03289

[22]     Shiraishi Y, Hirai T. Desulfurization of vacuum gas oil based on chemical oxidation followed by liquid− liquid extraction. Energy & Fuels. 2004 Jan 21;18(1):37-40. https://doi.org/10.1021/ef0301396

[23]     Humadi JI, Nawaf AT, Jarullah AT, Ahmed MA, Hameed SA, Mujtaba IM. Design of new nano-catalysts and digital basket reactor for oxidative desulfurization of fuel: Experiments and modelling. Chemical Engineering Research and Design. 2023 Feb 1;190:634-50. https://doi.org/10.1016/j.cherd.2022.12.043

[24]     Mahmood Q. Performance of tin oxide supported on reduced graphene oxide for oxidative desulfurization. El-Cezeri. 2023 May 5;10(2):284-95. https://doi.org/10.31202/ecjse.1210453

[25]     Hameed SA, Nawaf AT, Mahmood QA, Abdulateef LT, Jarullah AT, Mujtaba IM. Production of Green Fuel: A Digital Baffle Batch Reactor for Enhanced Oxidative Desulfurization of Light Gas Oil Using Nano-Catalyst. Iran. J. Chem. Chem. Eng. Research Article Vol. 2023;42(3). 10.30492/IJCCE.2022.547416.5138

[26]     Humadi JI, Gheni SA, Ahmed SM, Abdullah GH, Phan AN, Harvey AP. Fast, non-extractive, and ultradeep desulfurization of diesel in an oscillatory baffled reactor. Process Safety and Environmental Protection. 2021 Aug 1;152:178-87. https://doi.org/10.1016/j.psep.2021.05.028

[27]     Nawaf AT, Abdulmajeed BA. Design of oscillatory helical baffled reactor and dual functional mesoporous catalyst for oxidative desulfurization of real diesel fuel. Chemical Engineering Research and Design. 2024 Sep 1;209:193-209. https://doi.org/10.1016/j.cherd.2024.07.032

[28]     Nawaf AT, Gheni SA, Jarullah AT, Mujtaba IM. Optimal design of a trickle bed reactor for light fuel oxidative desulfurization based on experiments and modeling. Energy & Fuels. 2015 May 21;29(5):3366-76. https://doi.org/10.1021/acs.energyfuels.5b00157

[29]     Ahmed SM, Phan AN, Harvey AP. Mass transfer enhancement as a function of oscillatory baffled reactor design. Chemical Engineering and Processing-Process Intensification. 2018 Aug 1;130:229-39. https://doi.org/10.1016/j.cep.2018.06.016

[30]     Jafar SA, Nawaf AT, Humadi JI. Improving the extraction of sulfur-containing compounds from fuel using surfactant material in a digital baffle reactor. Materials Today: Proceedings. 2021 Jan 1;42:1777-83. https://doi.org/10.1016/j.matpr.2020.11.821

[31]     Mohammed ST, Gheni SA, Aqar DY, Hamad KI, Ahmed SM, Mahmood MA, Abdullah GH, Ali MK. Evaluation and optimal design of a high stability hydrothermal deoxygenation process

for production of green diesel fuel via deoxygenation of waste cooking oil. Process Safety and Environmental Protection. 2022 Mar 1;159:489-99. https://doi.org/10.1016/j.psep.2022.01.006

[32] Nawaf AT, Hamed HH, Hameed SA, Jarullah AT, Abdulateef LT, Mujtaba IM. Performance enhancement of adsorption desulfurization process via different new nano-catalysts using digital baffle batch reactor and mathematical modeling. Chemical Engineering Science. 2021 Mar 15;232:116384. https://doi.org/10.1016/j.ces.2020.116384

[33] Nawaf AT, Hameed SA, Abdulateef LT, Jarullah AT, Kadhim MS, Mujtaba IM. A novel synthetic nano-catalyst (Ag2O3/Zeolite) for high quality of light naphtha by batch oxidative desulfurization reactor. https://doi.org/10.9767/bcrec.16.4.11383.716-732

[34] Nawaf AT, Humadi JI, Jarullah AT, Ahmed MA, Hameed SA, Mujtaba IM. Design of nano-catalyst for removal of phenolic compounds from wastewater by oxidation using modified digital basket baffle batch reactor: experiments and modeling. Processes. 2023 Jul 1;11(7):1990. https://doi.org/10.3390/pr11071990

[35] Al-Dahhan M. Recent advances and scale-up of trickle bed reactors for energy and environmental applications. InProceedings of the International Symposium on Advances in Hydroprocessing of Oil Fractions (ISAHOF 2007) 2007 Jun 26 (pp. 26-29).

[36] Sachdeva TO, Pant KK. Deep desulfurization of diesel via peroxide oxidation using phosphotungstic acid as phase transfer catalyst. Fuel processing technology. 2010 Sep 1;91(9):1133-8. https://doi.org/10.1016/j.fuproc.2010.03.027

[37] Rezvani MA, Aghmasheh M. Synthesis and characterization of new nanocomposite TBA-PW11Ni@ NiO as an efficient and reusable heterogeneous catalyst in oxidative desulphurization of gasoline. Journal of the Taiwan Institute of chemical engineers. 2017 Aug 1;77:321-8. https://doi.org/10.1016/j.jtice.2017.05.014

[38] Shi Y, Fan M. Reaction kinetics for the catalytic oxidation of sulfur dioxide with microscale and nanoscale iron oxides. Industrial & engineering chemistry research. 2007 Jan 3;46(1):80-6. https://doi.org/10.1021/ie060889d